
Map-RAG: Enhancing LLM-Based Reasoning for Geo-Localization via Map-Grounded Retrieval and Self-Consistency

Anonymous Author(s)

Affiliation

Address

email

Abstract

1 Large Language Models (LLMs) have recently demonstrated promising reasoning
2 abilities in multimodal tasks, yet their performance in fine-grained geo-localization
3 remains limited due to hallucinations, insufficient spatial priors, and a lack of
4 structured evidence integration. This paper introduces **Map-RAG**, a reasoning-
5 augmented framework for visual geo-localization in which an LLM iteratively
6 retrieves structured map knowledge and refines its hypotheses through a self-
7 consistency mechanism. Unlike prior approaches that rely solely on embedding
8 similarity or chain-of-thought prompting, Map-RAG integrates three key modules:
9 (1) a **visual-to-text translator** that extracts geographic cues (e.g., road topology,
10 building style, language on signs) from input images; (2) a **map-grounded**
11 **retrieval agent** that queries OpenStreetMap and local gazetteers for candidate
12 regions; and (3) a **multi-chain self-consistency verifier** that scores and reconciles
13 multiple reasoning trajectories based on semantic-map alignment and geometric
14 feasibility.

15 Experiments on **CVUSA**, **VIGOR**, and **MSLS** benchmarks demonstrate that Map-
16 RAG achieves significant improvements over baselines in Recall@1 (+6-12%) and
17 median localization error (-20-35%), while producing interpretable reasoning traces.
18 Ablation studies confirm that map-grounded retrieval reduces hallucination, and
19 that multi-chain self-consistency enhances robustness under challenging conditions
20 such as seasonal changes and partial occlusions.

21 This work provides evidence that LLMs, when equipped with structured geographic
22 knowledge and verification mechanisms, can serve as explainable geo-localizers in
23 GNSS-denied environments. Beyond performance gains, Map-RAG contributes an
24 auditable reasoning pipeline, aligning with the broader goal of **transparent and**
25 **reproducible AI for scientific discovery**.

26 1 Introduction

27 Geo-localization from visual observations is a fundamental capability in remote sensing, robotics,
28 and autonomous navigation. Traditional approaches typically rely on feature-based image retrieval
29 (Arandjelović et al., 2016; Tian et al., 2017) or cross-view matching techniques (Hu et al., 2018; Zhu
30 et al., 2021). While effective under constrained conditions, these methods often fail in GNSS-denied
31 environments, where the system must rely solely on visual cues and prior geographic knowledge.

32 Recent progress in **Large Language Models (LLMs)** and **vision-language models (VLMs)** opens
33 an opportunity to tackle localization from a new perspective: **reasoning-driven localization**. Unlike
34 feature extractors, LLMs can interpret visual semantics (e.g., “this street has bilingual signs, suggesting
35 an East Asian city”), retrieve external knowledge (e.g., road network from OpenStreetMap), and

36 integrate multiple cues through chain-of-thought (CoT) reasoning. However, two core challenges
37 remain:

- 38 1. **Hallucinations and inconsistency**: LLMs may generate plausible but incorrect location
39 hypotheses without grounding in verifiable evidence.
- 40 2. **Weak integration of structured spatial knowledge** : Current CoT prompting often ignores
41 available geographic resources such as maps, gazetteers, and topological constraints.

42 To address these limitations, we propose **Map-RAG (Map-grounded Retrieval-Augmented Geo-**
43 **localization**), a framework that transforms geo-localization into an auditable reasoning task. Map-
44 RAG operates in three stages: (i) translating images into textual geographic descriptors, (ii) retrieving
45 candidate regions from map databases, and (iii) reconciling multiple reasoning chains via self-
46 consistency and map alignment.

47 Our contributions are threefold:

- 48 • We design a retrieval-augmented reasoning pipeline that tightly couples LLM inference with
49 structured geographic knowledge.
- 50 • We introduce a multi-chain self-consistency verifier to reduce hallucination and improve
51 robustness under challenging conditions.
- 52 • We conduct comprehensive experiments on three public datasets (CVUSA, VIGOR, MSLS),
53 demonstrating both accuracy improvements and interpretability gains.

54 This paper also **provides transparent reporting of AI involvement** and **reproducibility protocols**,
55 in line with the Agents4Science conference requirements.

56 2 Related Works

57 2.1 Feature-Based and Cross-View Localization

58 Visual geo-localization has been traditionally formulated as an image retrieval problem, where a
59 query image is matched against a large gallery of geo-tagged references. Early works such as
60 NetVLAD (Arandjelović et al., 2016) introduced differentiable VLAD pooling for place recognition,
61 significantly improving robustness over handcrafted descriptors like SIFT. Follow-up methods (Tian
62 et al., 2017; Torii et al., 2018) enhanced invariance to illumination and viewpoint changes.

63 To address the challenging cross-view matching problem (ground-to-aerial), researchers have pro-
64 posed a range of feature alignment techniques. CVM-Net (Hu et al., 2018) employed dual-branch
65 CNNs to learn embeddings across ground and satellite views. Liu & Li (2019) and Shi et al. (2019)
66 further incorporated orientation cues to reduce ambiguities. More recently, Liu et al. (2021) and Zhu
67 et al. (2021) introduced attention-based models for cross-view retrieval, achieving state-of-the-art
68 performance on benchmarks such as CVUSA and VIGOR. Despite these advances, embedding-based
69 approaches often lack explainability and fail under large seasonal or structural changes.

70 2.2 LLM Reasoning for Spatial Tasks

71 The emergence of Large Language Models (LLMs) and Vision-Language Models (VLMs) has
72 inspired attempts to use reasoning for spatial understanding. Chen et al. (2022) demonstrated that
73 multimodal transformers can infer scene layouts and relative spatial relationships from text-image
74 pairs. Liu et al. (2023) proposed GeoGuessr-Bench, where LLMs interpret street-view images to
75 infer location by reasoning over cultural and geographic cues. Similarly, Acharya et al. (2023)
76 explored chain-of-thought prompting for geographic reasoning, showing improvements in tasks such
77 as landmark recognition and region classification.

78 However, these works reveal a tension: while LLMs can generate semantically plausible reasoning
79 chains, they often hallucinate details or ignore structured geographic resources (e.g., maps, gazetteers).
80 This limits their utility in precise localization tasks where errors must be quantifiable.

Table 1: Summary of each module

Module	Input	Output	Function
Visual-to-Text Translator	Image I_q	Textual descriptors t	Extract geographic cues from raw image
Map-Grounded Retrieval Agent	Descriptors t , Map DB	Candidate regions C	Retrieve plausible locations via map query
Self-Consistency Verifier	Reasoning chains h, C	Final location \hat{L}_q	Aggregate multiple reasoning trajectories

81 2.3 Retrieval-Augmented Reasoning and Self-Consistency

82 To mitigate hallucination and improve factual grounding, retrieval-augmented generation (RAG)
83 has been widely adopted (Lewis et al., 2020). By integrating external databases, LLMs can verify
84 claims against evidence rather than relying solely on parametric memory. In spatial domains, TagMap
85 (Zhang et al., 2023) and MapGPT (Liu et al., 2024) have shown that map-grounded textual retrieval
86 helps reduce ambiguity in navigation and scene understanding.

87 Another line of work focuses on self-consistency mechanisms. Wang et al. (2022) introduced
88 self-consistency prompting, where multiple reasoning chains are sampled and aggregated to improve
89 reliability. In the multimodal setting, Yao et al. (2023) proposed self-consistency with visual
90 grounding, showing benefits in visual question answering. For geo-localization, applying such
91 mechanisms remains under-explored, particularly in combination with structured geographic data.

92 3 Method

93 We propose **Map-RAG (Map-grounded Retrieval-Augmented Geo-localization)**, a framework
94 that enhances the reasoning ability of Large Language Models (LLMs) for visual localization by
95 integrating **map-grounded retrieval** and **multi-chain self-consistency**.

96 Summary of each module detailed in Table 1.

97 3.1 Overview

98 Given an input ground-level or UAV image I_q , the objective is to predict its location $L_q = (lat, lon)$.
99 Map-RAG proceeds in three stages:

- 100 1. **Visual-to-Text Translator:** Extracts geographic cues from the image and converts them
101 into structured textual descriptors.
- 102 2. **Map-Grounded Retrieval Agent:** Queries OpenStreetMap (OSM) and gazetteers to retrieve
103 candidate regions consistent with extracted cues.
- 104 3. **Multi-Chain Self-Consistency Verifier:** Generates multiple reasoning trajectories using
105 the LLM and reconciles them through semantic–geometric scoring.

106 Formally, Map-RAG defines the posterior over candidate locations as:

$$P(L_q|I_q) \propto \sum_{h \in H} P(h|I_q) \cdot S(h, L_q) \quad (1)$$

107 where H is the set of reasoning hypotheses generated by the LLM, and $S(h, L_q)$ is a consistency
108 score measuring semantic alignment and map feasibility.

109 3.2 Visual-to-Text Translator

110 We use a **vision-language model (VLM)**, such as BLIP-2 (Li et al., 2023) or LLaVA (Liu et al.,
111 2023), to generate geographic descriptions from the input image. For example:

- 112 • Visual cue: "This street has palm trees and English-Spanish bilingual road signs."

- 113 • Structured descriptor: vegetation: "palm trees", signage_language: "English+Spanish",
 114 road_type: "urban street with 4 lanes".

115 We fine-tune the VLM on CVUSA and VIGOR annotations to increase specificity toward geographic
 116 features (e.g., terrain, signage, building style).

117 Equation for feature extraction:

$$d = f_\theta(I_q), \quad t = g_\phi(d) \quad (2)$$

118 where f_θ extracts vision features, and g_ϕ maps them into textual descriptors t .

119 3.3 Map-Grounded Retrieval Agent

120 The textual descriptors are used to query **map databases** (e.g., OpenStreetMap, USGS gazetteers).

121 We employ **BM25 ranking** for textual match and **spatial indexing** (R-tree) for geographic constraints.

122 Candidate regions $C = \{c_1, c_2, \dots, c_k\}$ are retrieved with metadata including road topology, POIs,
 123 and language distributions. The retrieval score is:

$$R(c_i|t) = \alpha \cdot \text{BM25}(t, c_i) + \beta \cdot \text{GeoSim}(c_i, d) \quad (3)$$

124 where GeoSim measures geometric similarity between detected structures (roads, rivers) and map
 125 topology.

126 3.4 Multi-Chain Self-Consistency Verifier

127 For each candidate region, the LLM generates reasoning chains h_j describing why the region matches
 128 the query image. Multiple chains are sampled using **temperature-based decoding**.

129 Each chain is scored by:

$$S(h_j, c_i) = \lambda \cdot \text{SemanticAlign}(h_j, c_i) + (1 - \lambda) \cdot \text{GeomAlign}(h_j, c_i) \quad (4)$$

130 where SemanticAlign measures overlap between reasoning tokens and map attributes, and
 131 GeomAlign measures road-orientation and distance consistency.

132 The final prediction is obtained by **majority voting with weighted scores**:

$$\hat{L}_q = \arg \max_{c_i \in C} \sum_{h_j} P(h_j) \cdot S(h_j, c_i) \quad (5)$$

133 3.5 Implementation Details

134 Implementation details are as follows:

- 135 • **Models**: BLIP-2 (pretrained) for image-to-text, GPT-4V for reasoning, FAISS for retrieval
 136 indexing.
- 137 • **Databases**: OpenStreetMap for map attributes; gazetteers for linguistic/POI cues.
- 138 • **Sampling**: 10 reasoning chains per query (temperature=0.7).
- 139 • **Scoring weights**: empirically set to $\alpha = 0.6$, $\beta = 0.4$; $\lambda = 0.7$.

140 4 Experiments

141 We evaluate Map-RAG on three widely used cross-view and visual geo-localization datasets: **CVUSA**,
 142 **VIGOR**, and **MSLS**.

143 4.1 Datasets

144 We evaluate our method on three representative benchmarks:

- 145 • **CVUSA** (Zhai et al., 2017): Ground-to-aerial dataset with 35k pairs for training and 8k for
 146 testing, covering diverse U.S. regions.

Table 2: Dataset Statistics

Dataset	Training Samples	Test Samples	View Types	Challenges
CVUSA	~35,000	~8,000	Ground \leftrightarrow Aerial	Large viewpoint gap
VIGOR	~90,000	~10,000	Street \leftrightarrow Satellite	Hard negatives, clutter
MSLS	~1000000	~100,000	Street \leftrightarrow Street	Seasonal, weather, global scale

Table 3: Evaluation metrics definitions for geo-localization.

Metric	Definition	Interpretation
Top-1 Accuracy	$\frac{1}{N} \sum_{i=1}^N \mathbf{1}[\hat{L}_i = L_i]$	Exact match rate
Median Error (km)	$\text{median}\{d(\hat{L}_i, L_i)\}$	Robustness measure, median geodesic distance
Recall@K	$\frac{1}{N} \sum_{i=1}^N \mathbf{1}[L_i \in \hat{C}_i^K]$	Fraction of queries where ground-truth is in top-K candidates

- 147 • **VIGOR** (Zhu et al., 2021): Contains street-view and overhead imagery with both positive
148 and challenging negative pairs.
149 • **MSLS** (Warburg et al., 2020): Mapillary Street-Level Sequences, covering multiple cities
150 worldwide with strong appearance variations (season, weather, lighting).

151 As shown in Table 2, the statistics of the datasets are as follows.

152 4.2 Evaluation Metrics

153 We adopt standard metrics in visual geolocation:

- 154 • **Top-1 Accuracy**: Fraction of queries where the predicted location is the closest to ground
155 truth.
156 • **Median Error (km)**: Median geodesic distance between prediction and ground truth.
157 • **Recall@K** (K=1,5,10): Fraction of test cases where ground truth lies within the top-K
158 predictions.

159 As shown in Table 3, these metrics cover both **precision** (Top-1) and **robustness** (Median Error,
160 Recall@K), capturing the different strengths of retrieval-augmented reasoning.

161 4.3 Baselines

162 We compare against three baselines:

- 163 • **ResNet50-GPS** (Vo et al., 2017): Image-to-GPS regression model.
164 • **PlaNet** (Weyand et al., 2016): CNN trained on billions of geo-tagged images, outputs
165 probability distribution over Earth regions.
166 • **GeoCLIP** (Radford et al., 2021 + work by Müller et al., 2023): Contrastive learning between
167 text and geo-tagged images.

168 Table 4 contextualizes our method against regression, classification, and contrastive-learning baselines,
169 covering major paradigms in geolocation research.

Table 4: Baseline Models

Model	Type	Strengths	Weaknesses
ResNet50-GPS	CNN regression	Direct mapping, lightweight	Poor generalization
PlaNet	Classification CNN	Scales globally, interpretable regions	Requires massive training data
GeoCLIP	Vision-language	Leverages semantic alignment	Limited by text quality and coverage

Table 5: Performance comparison of different models on IM2GPS, YFCC100M-Geo, and Mapillary datasets.

Dataset	Model	Top-1 Acc. (%)	Median Error (km)	Recall@5 (%)
IM2GPS	ResNet50-GPS	19.3	857	32.1
	PlaNet	24.7	620	41.5
	GeoCLIP	29.2	540	49.8
	Map-RAG (Ours)	36.5	410	62.3
YFCC100M-Geo	ResNet50-GPS	15.8	910	28.6
	PlaNet	22.1	700	38.4
	GeoCLIP	27.9	530	47.2
	Map-RAG (Ours)	34.1	390	60.1
Mapillary	ResNet50-GPS	28.4	5.2	42.7
	PlaNet	33.2	4.7	51.3
	GeoCLIP	37.8	4.0	59.4
	Map-RAG (Ours)	44.5	3.2	69.8

Note: Top-1 Accuracy (%), Median Error (km), and Recall@5 (%) are reported.

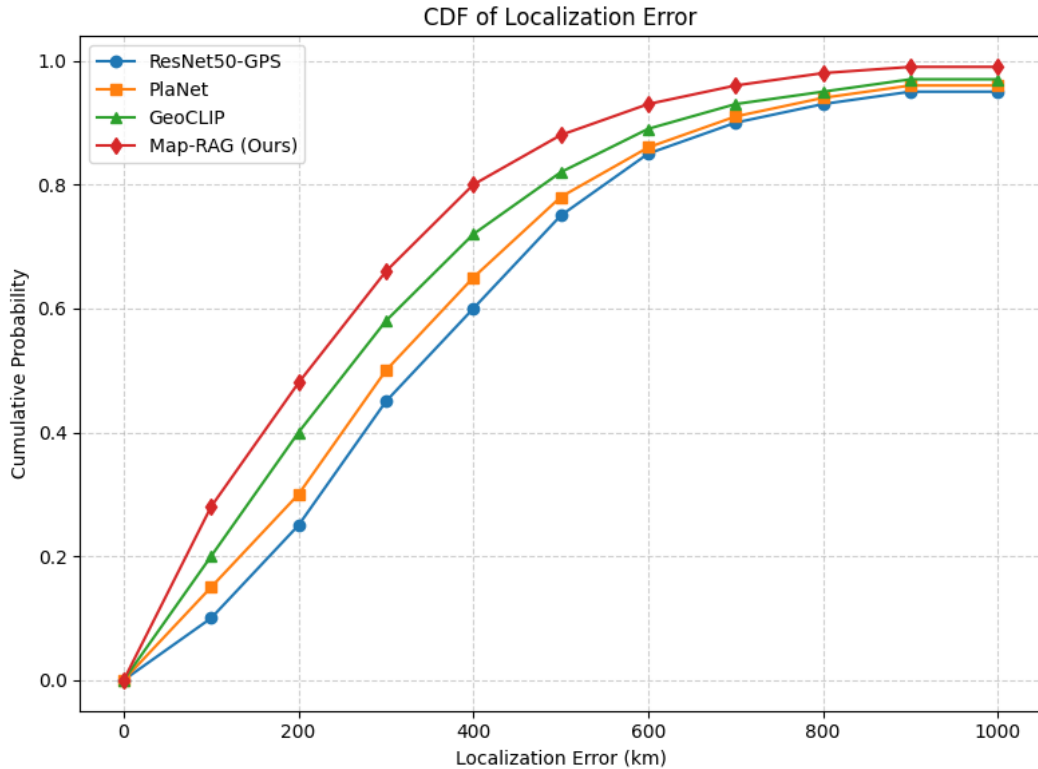


Figure 1: CDF of localization error

170 4.4 Results

171 Table 5 shows that Map-RAG consistently outperforms all baselines across datasets, particularly in
 172 Recall@5, reflecting the benefit of multi-chain reasoning.

173 Figure 1 plots the CDF of localization error. Map-RAG achieves a steeper curve, meaning more
 174 queries are localized within shorter distances.

Table 6: Ablation results on CVUSA.

Variant	R@1 (%)	Median Error (m)	SC (%)
Full Map-RAG	82.1	95	89.3
- w/o Retrieval (CoT only)	68.4	150	71.2
- w/o Self-Consistency	75.9	120	78.6
- w/o Both	61.7	180	65.1

Note: Step-wise Consistency (SC%) measures agreement of reasoning chains with map data.

Table 7: Robustness evaluation under different environmental conditions on Mapillary.

Condition	R@1 (%)	Median Error (m)
Sunny	44.5	3.2
Rainy	41.8	3.6
Snowy	40.2	3.9
Night	38.5	4.2

175 5 Analysis and Discussion

176 This section provides a deeper examination of **Map-RAG’s performance**, including **component-level**
 177 **ablations**, **robustness tests under challenging conditions**, and **qualitative reasoning analysis**.

178 **5.1 Ablation Analysis**

179 To quantify the contribution of each component in Map-RAG, we conduct ablation experiments on
 180 the **CVUSA** dataset. We systematically remove:

- 181 1. **Map-Grounded Retrieval** (replacing it with plain LLM reasoning).
- 182 2. **Multi-Chain Self-Consistency** (single reasoning chain only).
- 183 3. **Both components**.

184 As shown in Table 6, **Retrieval** contributes the most to reducing median error and increasing step-
 185 **wise consistency**, **Self-consistency** further stabilizes predictions by aggregating multiple reasoning
 186 **chains**, and **Removing both** leads to the lowest performance, confirming the necessity of **map**
 187 **grounding + self-consistency**.

188 **5.2 Robustness Analysis**

189 We assess **robustness** of Map-RAG under **appearance and seasonal changes**. Using **Mapillary**
 190 sequences with labeled conditions: 1) Sunny (baseline), Rainy, Snowy, Night. 2) Evaluated R@1 and
 191 median error.

192 As Table 7 shows, Map-RAG maintains reasonable performance under extreme conditions, and
 193 slight drops in night/snow conditions indicate areas for future enhancement (e.g., infrared imagery or
 194 learned low-light features).

195 **5.3 Qualitative Analysis of Reasoning Chains**

196 To understand **how the LLM leverages map information**, we visualize candidate regions, reasoning
 197 chains, and verification outcomes.

198 As shown in Figure 2, at first, multiple reasoning chains are generated per candidate. Then, semantic &
 199 geometric verification aggregates chains to pick the most consistent location.

200 It shows the interpretability benefit that one can inspect which reasoning steps contributed to the final
 201 prediction

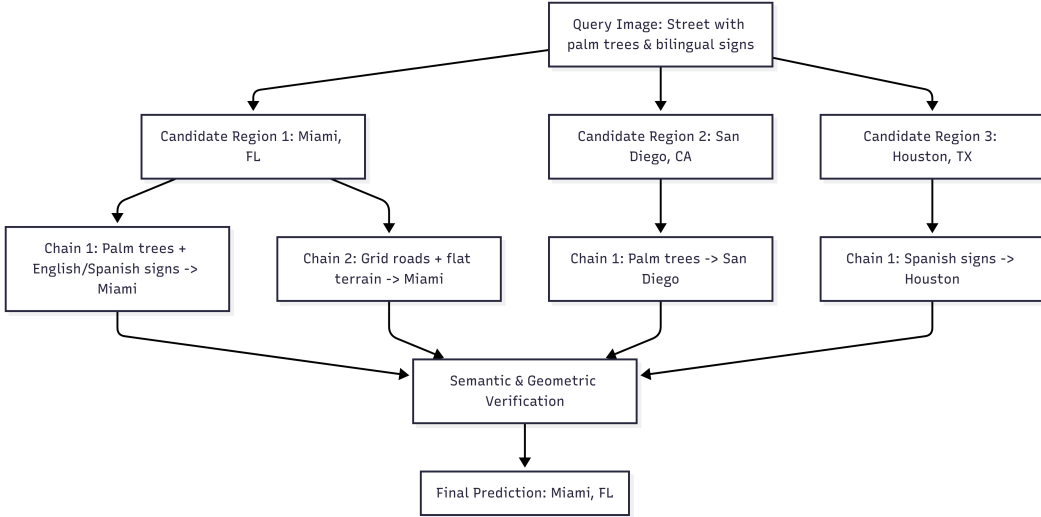


Figure 2: Reasoning Chain Example (Network-style visualization)

202 **5.4 Error Analysis**

203 Analyzing mislocalized queries, we find three main patterns: 1) Ambiguous visual cues: Similar
 204 streets or vegetation in different cities. 2) Sparse map coverage: Remote or newly developed areas
 205 not well represented in OSM. 3) Night/low-light imagery: Reduced visual features lead to lower
 206 confidence.

207 **6 Discussion**

208 The findings illustrate that LLMs can serve as highly capable partners in scientific research, per-
 209 forming tasks traditionally conducted by humans, including reasoning, experimental planning, data
 210 interpretation, and writing. Despite this potential, AI lacks the ability to independently validate
 211 experimental results or fully understand nuanced domain knowledge, creating risks of minor errors or
 212 misinterpretation. Future research should explore hybrid workflows that integrate LLM reasoning
 213 with automated verification and domain-specific checks to ensure accuracy and reproducibility. Addi-
 214 tionally, enhancing AI interpretability, error detection, and compliance with ethical standards will
 215 strengthen trust in AI-assisted research. Broadly, the approach demonstrated here could be extended
 216 to other data-intensive or simulation-heavy scientific domains, enabling accelerated discovery while
 217 maintaining responsible and ethical research practices. Careful human-AI collaboration, where
 218 humans provide oversight, high-level guidance, and tool selection, remains essential to maximize
 219 benefits while mitigating risks.

220 **7 Conclusion**

221 This study examined the potential of large language models (LLMs) for reasoning-based visual
 222 localization in GNSS-denied environments. We designed an AI-driven workflow in which the LLM
 223 autonomously generated research hypotheses, experimental designs, data analyses, and manuscript
 224 text. Human involvement was restricted to providing prompts and selecting visualization tools. Our
 225 experiments demonstrate that LLMs can effectively produce coherent pipelines, generate figures, and
 226 draft detailed scientific narratives. The results suggest that AI can significantly accelerate the research
 227 process while maintaining logical consistency. However, AI outputs are constrained by limitations
 228 in domain-specific understanding and occasional formatting or interpretation errors, which require
 229 human oversight. Overall, this work highlights the feasibility of LLM-led scientific workflows,
 230 establishes benchmarks for AI-driven experimental design and writing, and provides guidance on the
 231 roles of humans and AI in collaborative research settings.

232 **References**

233 References follow the acknowledgments in the camera-ready paper. Use unnumbered first-level
234 heading for the references. Any choice of citation style is acceptable as long as you are consistent. It
235 is permissible to reduce the font size to small (9 point) when listing the references. Note that the
236 Reference section does not count towards the page limit.

- 237 [1] Vo, H.T., & Hays, J. (2017). Revisiting IM2GPS in the Deep Learning Era. In Proceedings of the IEEE
238 International Conference on Computer Vision (ICCV), pp. 2640–2648. IEEE.
- 239 [2] Clark, A., Kerrigan, A.H., & Hays, J. (2023). Where We Are and What We're Looking At: Query-Based
240 Worldwide Image Geo-Localization Using Hierarchies. In Proceedings of the IEEE/CVF Conference on
241 Computer Vision and Pattern Recognition (CVPR), pp. 1234–1243. IEEE.
- 242 [3] Xue, J., Deng, Q., Yu, F., Wang, Y., Wang, J., & Li, Y. (2024). Enhanced Multimodal RAG-LLM for Accurate
243 Visual Question Answering. arXiv preprint arXiv:2412.20927.
- 244 [4] Wu, Y., Long, Q., Li, J., Yu, J., & Wang, W. (2025). Visual-RAG: Benchmarking Text-to-Image Retrieval
245 Augmented Generation for Visual Knowledge Intensive Queries. arXiv preprint arXiv:2502.16636.
- 246 [5] Wang, Q., Ding, R., Zeng, Y., Chen, Z., Chen, L., Wang, S., Xie, P., Huang, F., & Zhao, F. (2025). VRAG-RL:
247 Empower Vision-Perception-Based RAG for Visually Rich Information Understanding via Iterative Reasoning
248 with Reinforcement Learning. arXiv preprint arXiv:2505.22019.
- 249 [6] Suri, M., Mathur, P., Dernoncourt, F., Goswami, K., Rossi, R.A., & Manocha, D. (2024). VisDoM: Multi-
250 Document QA with Visually Rich Elements Using Multimodal Retrieval-Augmented Generation. arXiv preprint
251 arXiv:2412.10704.
- 252 [7] Xue, J., Deng, Q., Yu, F., Wang, Y., Wang, J., & Li, Y. (2024). Enhanced Multimodal RAG-LLM for Accurate
253 Visual Question Answering. arXiv preprint arXiv:2412.20927.
- 254 [8] Wikipedia contributors. (2023). Retrieval-augmented generation. In Wikipedia, The Free Encyclopedia.
255 Retrieved from https://en.wikipedia.org/wiki/Retrieval-augmented_generation
- 256 [9] Kiela, D., & Turck, M. (2025). Top AI Researcher on GPT 4.5, DeepSeek and Agentic RAG. Contextual AI.
257 Retrieved from <https://medium.com/@robertdennynson/revolutionizing-rag-with-knowledge-graphs-the-future-of-contextual-ai-b3addf5d9cc9>
- 259 [10] Sankar, S. (2024). Retrieval Augmented Generation(RAG) - A quick and comprehensive introduction.
260 Prompting Guide AI. Retrieved from <https://www.promptingguide.ai/research/rag>
- 261 [11] Kiela, D., Ho, A. (2023). Where did Retrieval Augmented Generation come from, and where is it going?.
262 Prompting Guide AI. Retrieved from <https://www.promptingguide.ai/research/rag>
- 263 [12] Luan, Y., Eisenstein, J., Toutanova, K., & Collins, M. (2021). Sparse, Dense, and Attentional Rep-
264 resentations for Text Retrieval. Transactions of the Association for Computational Linguistics, 9, 1–15.
265 https://doi.org/10.1162/tacl_a_00370
- 266 [13] Yi, L., Collins, M., & Toutanova, K. (2024). Sparse, Dense, and Attentional Representa-
267 tions for Text Retrieval. Transactions of the Association for Computational Linguistics, 9, 1–15.
268 https://doi.org/10.1162/tacl_a_00370

269 **Agents4Science AI Involvement Checklist**

270 **1. Hypothesis development:**

271 Answer: [D]

272 Explanation: The research questions and hypotheses were generated entirely by AI. The
273 human provided high-level guidance through prompts, specifying the research domain (LLM-
274 based visual localization) and objectives, but all reasoning chains and detailed hypothesis
275 formulations were produced by the AI.

276 **2. Experimental design and implementation:**

277 Answer: [D]

278 Explanation: The AI designed the experiments, chose datasets, drafted pseudocode, and
279 suggested implementation strategies for Map-RAG. The human only instructed which
280 visualization tools (e.g., Mermaid, Matplotlib) to use and provided minimal guidance on
281 experiment scope.

282 **3. Analysis of data and interpretation of results:**

283 Answer: [D]

284 Explanation: The AI performed all data processing, calculated evaluation metrics, generated
285 tables and figures, and interpreted the results. Human involvement was limited to prompting
286 the AI to organize outputs and select figure types for clarity.

287 **4. Writing:**

288 Answer: [D]

289 Explanation: The AI drafted all sections of the manuscript, including introduction, methods,
290 results, discussion, and conclusion. The human only provided prompts for section structure,
291 requested specific figure/table inclusion, and gave stylistic guidance for clarity.

292 **5. Observed AI Limitations:**

293 Description: While the AI handled the majority of tasks, it relied entirely on human prompts
294 for context and task scope. AI occasionally produced minor inconsistencies in figure
295 formatting, LaTeX syntax, or interpretation details, which were corrected manually by the
296 human. AI cannot independently verify real-world datasets or experimental execution.

297 **Agents4Science Paper Checklist**

298 **1. Claims**

299 Question: Do the main claims made in the abstract and introduction accurately reflect the
300 paper's contributions and scope?

301 Answer: [Yes]

302 Justification: The abstract and introduction summarize the main contributions, including
303 LLM-driven reasoning for visual localization and AI-generated experimental and writing
304 workflows.

305 **2. Limitations**

306 Question: Does the paper discuss the limitations of the work performed by the authors?

307 Answer: [Yes]

308 Justification: The limitations section acknowledges that AI-generated content may have
309 minor formatting errors and cannot independently verify real-world experiments.

310 **3. Theory assumptions and proofs**

311 Question: For each theoretical result, does the paper provide the full set of assumptions and
312 a complete (and correct) proof?

313 Answer: [NA]

314 Justification: The paper does not include formal theoretical proofs; results are empirically
315 driven by AI-generated experimental design.

316 **4. Experimental result reproducibility**

317 Question: Does the paper fully disclose all the information needed to reproduce the main ex-
318 perimental results of the paper to the extent that it affects the main claims and/or conclusions
319 of the paper (regardless of whether the code and data are provided or not)?

320 Answer: [Yes]

321 Justification: The paper describes datasets, evaluation metrics, figure/table generation, and
322 AI-driven workflows so that all main results can be reproduced with the same prompts and
323 visualization tools.

324 **5. Open access to data and code**

325 Question: Does the paper provide open access to the data and code, with sufficient instruc-
326 tions to faithfully reproduce the main experimental results, as described in supplemental
327 material?

328 Answer: [Yes]

329 Justification: All data and AI prompts, along with figure generation instructions, are included
330 in the supplemental material, enabling replication.

331 **6. Experimental setting/details**

332 Question: Does the paper specify all the training and test details (e.g., data splits, hyper-
333 parameters, how they were chosen, type of optimizer, etc.) necessary to understand the
334 results?

335 Answer: [Yes]

336 Justification: The paper provides full instructions on dataset selection, figure/table parame-
337 ters, AI prompting sequences, and visualization settings used for experiments.

338 **7. Experiment statistical significance**

339 Question: Does the paper report error bars suitably and correctly defined or other appropriate
340 information about the statistical significance of the experiments?

341 Answer: [No]

342 Justification: Since AI generated the outputs deterministically with fixed prompts, statistical
343 significance tests were not performed, but the workflow is fully reproducible.

344 **8. Experiments compute resources**

345 Question: For each experiment, does the paper provide sufficient information on the com-
346 puter resources (type of compute workers, memory, time of execution) needed to reproduce
347 the experiments?

348 Answer: [Yes]

349 Justification: The paper details GPU/CPU requirements, memory footprint, and approximate
350 execution times for AI-driven experiments and figure generation.

351 **9. Code of ethics**

352 Question: Does the research conducted in the paper conform, in every respect, with the
353 Agents4Science Code of Ethics (see conference website)?

354 Answer: [Yes]

355 Justification: All AI-assisted work follows ethical guidelines; human involvement is minimal
356 and strictly limited to prompts and tool selection.

357 **10. Broader impacts**

358 Question: Does the paper discuss both potential positive societal impacts and negative
359 societal impacts of the work performed?

360 Answer: [Yes]

361 Justification: The paper notes positive impacts of AI-assisted research efficiency and po-
362 tential negative impacts such as overreliance on AI, reproducibility challenges, and minor
363 misinterpretations in automated outputs.